CIRP Annals - Manufacturing Technology 72 (2023) 497–500

Contents lists available at ScienceDirect

CIRP Annals - Manufacturing Technology

journal homepage: https://www.editorialmanager.com/CIRP/default.aspx

What can micromechanics tell us about the surface integrity of shot-peened materials?

Jose A. Robles-Linares[a], Gonzalo García Luna[a,b], Andrea la Monaca[a,b], Zhirong Liao (2)[a,*], Mark C. Hardy[b]

[a] Rolls-Royce UTC in Manufacturing and On-Wing Technology, Faculty of Engineering, University of Nottingham, Nottingham, United Kingdom
[b] Rolls-Royce plc, Derby, United Kingdom

ARTICLE INFO

Article history:
Available online 27 April 2023

Keywords:
Surface integrity
Nickel alloy
Micromechanics

ABSTRACT

Standard techniques for assessing shot peening include XRD and EBSD for measuring residual stresses and severe deformation beneath the surface; however, these techniques do not consider the localised micromechanical behaviour. Here, single-grain micropillar compression tests in a Ni-base superalloy reveal that the micromechanical effect of shot peening could be insignificant due to the machining-induced pre-strained condition of the surface. Further, it is shown that shot-peening-induced strengthened layer can extend much less (~50%) than the depth at which compressive stresses are still present. This work highlights the need for employing micromechanics as a complementary shot peening assessment technique for machined components.

1. Introduction

The challenging environment inside aeroengines demands for ever-stronger materials that can withstand high temperatures whilst maintaining superior mechanical properties. Polycrystalline Ni-base superalloys, consisting of an FCC gamma (γ) matrix that is precipitation-hardened with a gamma prime (γ') phase, pose an attractive solution due to their resilient yield strength, and resistance to fatigue, creep and crack growth at high temperatures [1,2]. However, these materials are difficult to machine, and thus, subsurface microstructural alterations can be induced in the form of grain refinement, deformed γ' precipitates, tensile residual stresses, and mechanical twins [3,4]. The latter is of significant importance given that the high-angle boundary of twins impede dislocation motion and thus act as stress concentrators [5], which ultimately enables crack initiation.

Multiple studies regarding the surface integrity of as-machined Ni-base superalloys exist [3,6]; these have shown the complex role played by cutting temperatures on local lattice reconfiguration [7], showing that a controlled set of thermal conditions could allow for higher temperatures to actually reduce the machining-induced subsurface deformation [8] by increasing thermal softening and shear localisation. Furthermore, the recrystallised layer on machined Ni-base superalloys has also been characterised via micromechanical testing, showing that it possesses a dominant plastic (i.e., rather than elastic) behaviour even at low strains, which is detrimental for fatigue life [9]. Simulation-based methods (e.g., crystal plasticity, molecular dynamics or contact mechanics) have been explored for predicting the behaviour of these alloys (e.g., [5,10]), but they are usually confined to the bulk material, which lacks to capture the behaviour beneath the material's outermost surface (i.e., where severe deformation exists).

These intricacies, along with machining-induced tensile stresses, calls for the need of a post-processing technique that improves the in-life performance of the component. Shot peening is a commonly used method for this that consists of continuously impacting the material's surface with shots, which induces a compressive stress profile in the subsurface [9] (Fig. 1). The impact-induced forest of dislocations in the crystal lattice of the superficial layer improves the material's performance due to the strain hardening effect associated with the localised plastic deformation [11]. Thus, the resistance to deformation in the superficial layer of the shot-peened surface can be expected to be larger than in the bulk material, and therefore aid in the fatigue strength of the material. But how can the reach of shot peening be assessed?

The effect of shot peening is measured by evaluating the material condition beneath the shot-peened surface, with a focus on plastic

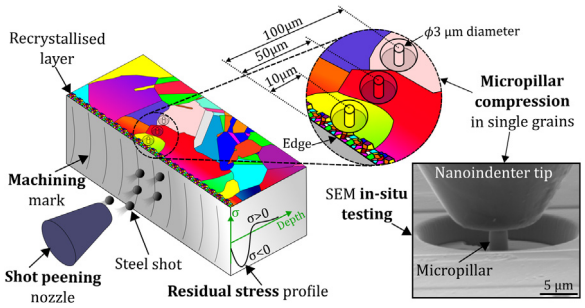

Fig. 1. Proposed methodology for assessing the integrity of the as-machined and shot-peened Ni-base superalloy with micromechanics.

* Corresponding author.
E-mail address: Zhirong.Liao@nottingham.ac.uk (Z. Liao).

https://doi.org/10.1016/j.cirp.2023.04.003

deformation depth and residual stresses. Traditionally, various material analysis techniques are used for this: scanning electron microscopy (SEM); microhardness testing; x-ray diffraction (XRD), which permits to obtain the residual stress profile beneath the surface and to quantify the depth of plastic deformation (i.e., the strain hardening depth, captured by means of peak broadening); and electron backscatter diffraction (EBSD), which after data post-processing yields the geometrically necessary dislocation (GND) density. However, caution must be employed with these techniques since, for instance, microhardness measurements near the edge are not reliable [12]; residual stresses can be significantly relieved after a single cycle of fatigue loading (e.g., 60% relaxation after 1 cycle with 1.2% strain [13]); and GND density does not capture the large strains that take place via homogeneous slipping along a given slip system of the crystal [11]. Thus, more advanced techniques, such as micromechanical testing (Fig. 1), are required [14] for providing richer near-edge data in terms of stress-strain.

Here, micromechanical analysis (i.e., micropillar compression) is employed as an assessment technique in shot-peened specimens (Fig. 1) of a machined Ni-base superalloy, and it is shown that the larger dislocation density achieved by an increased shot peening intensity could be positive for the material by a significant increase of the critical resolved shear stress (CRSS), but it is also noted that given the pre-strained condition (i.e. machined surface), peening does not always pose a material enhancement scenario and could have a negligible effect on the material's CRSS. More importantly, it is proved that even while the residual stress profile may show a large depth of shot peening action, micromechanical strength (i.e., yield strength, CRSS) could be affected significantly less.

2. Experimental details

To investigate the role of shot peening on pre-strained (i.e., machined) surfaces, a micromechanics-based study has been conducted on a next-generation polycrystalline Ni-base superalloy under development by Rolls-Royce plc [15], with a 51–53 vol% γ' fraction and ASTM 8 to 7 average grain size (Fig. 2).

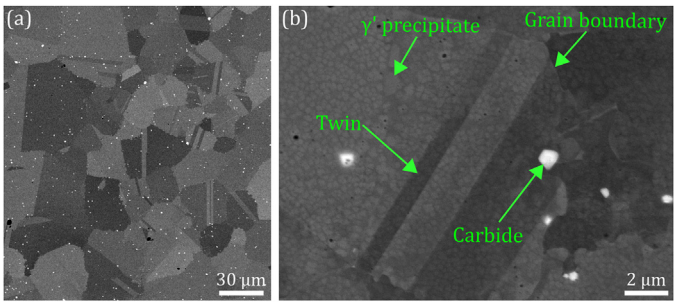

Fig. 2. Microstructure of the investigated Ni-base superalloy. (a) SEM image depicting the grain structure and, (b) close-up view.

The material was machined via turning and it was subsequently shot-peened to achieve a 125% coverage with two different intensities. Thus, three material conditions were considered: (i) as-machined ('AM'), (ii) machined and shot-peened at a low intensity ('AM+LowPI'), and (iii) machined and shot-peened at a large intensity ('AM+LargePI'). The alloy was produced, machined and shot-peened by Rolls-Royce plc.

The samples were cut and polished to make them of suitable size, shape, and quality for SEM, XRD, and micromechanical testing.

EBSD was employed in near-edge locations to identify suitable micromechanical testing locations. Focused Ion Beam (FIB) milling was employed to produce micropillars beneath the machined/peened surface at three depths: (i) at the edge, (ii) at 50 µm, and (iii) at 100 µm (Fig. 1). Micropillars were ensured to be located fully inside single grains and had a nominal diameter of 3 µm and aspect ratio of 3:1 [16].

The micropillars were subsequently compressed at a constant strain rate of 0.01 s^{-1} with a flat punch diamond tip (Synton-MDP, Switzerland) using an in-situ nanoindenter (Alemnis, Switzerland) inside an SEM, and tests were stopped after a 0.1 strain (non-corrected) was achieved. Results were analysed by an in-house Matlab code to obtain engineering stress-strain data.

3. Role of shot peening on the metallurgy of the alloy

A traditional shot peening assessment was performed by means of XRD to obtain the residual stress profiles and the strain hardening depths (Fig. 3). As expected, the AM condition depicted large tensile stresses near the surface, having a very similar strain hardening depth as the AM+LowPI condition (Fig. 3b), roughly normalising at around a 100 µm depth. Nevertheless, it is easy to note that the AM +LargePI condition exhibited the largest compressive residual stress profile (Fig. 3a) and achieved a deeper strain hardening depth than in the other two conditions given the increased deformation related to the larger peening intensity. Consequently, based solely on this, peening at the larger intensity appears to perform better than the low intensity, as it shows evidence that the surface will be 'enhanced' up to depths that are close to 200 µm deep (Fig 3b).

To complement the analysis, the samples were assessed with EBSD (Fig. 4a-c). The crystallographic analysis shows that the AM and AM+LargePI have more pronounced grain sweeping and intragrain

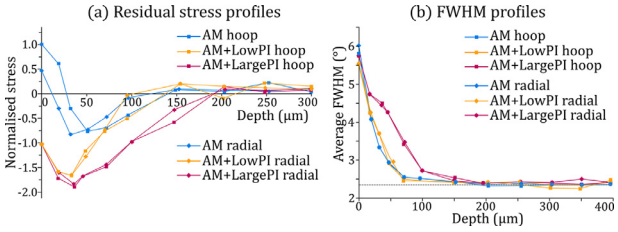

Fig. 3. Residual stresses and full width at half maximum (FWHM) profiles for each surface condition.

misorientation than in the AM+LowPI condition, implying perhaps that the lower peening intensity is only useful for balancing the effect of the tensile residual strains due to machining, but not enough to induce further deformation into the material. Analysing the GND density (Fig. 4d-f), it can easily be noted that even while there is a larger number of dislocations near the edge for the AM condition (Fig. 4d), the overall deformed layer (DL) depth is larger for the AM +LargePI condition, reaching 36 µm deep beneath the surface, while it is significantly lower for the AM+LowPI condition (11 µm deep). However, while this type of crystallographic analysis is useful for partially quantifying the effect of shot peening, it fails to capture the dislocation concentrated in compact shear bands [11], where large dislocations can occur without accumulating significant strains. On

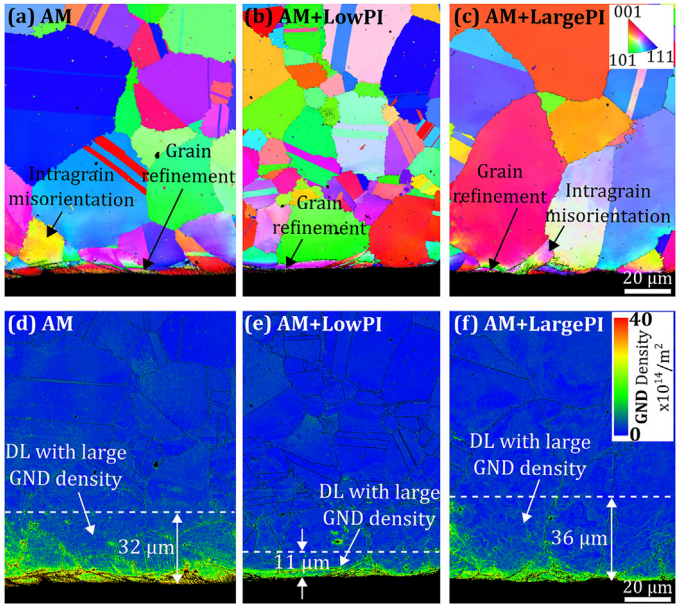

Fig. 4. Microstructure beneath the machined and peened surfaces (processed surfaces at the bottom). (a-c) EBSD maps (IPF Y) near the surface show the grain refinement zone and grain sweeping, and (d-e) GND density maps in the same locations depict the deformed layer (DL) depths.

the other hand, due to resolution limitation, the EBSD technique would normally miss to capture the localised dislocation activities.

To complement the EBSD and GND density information, backscatter electron imaging (BSEI) was also employed to examine the subsurface since it allows for ease of visualisation of lattice defects (e.g., dislocations, stacking faults) near the surface of the sample (Fig. 5). With this technique, it was found that the DL (i.e., depicting large intragranular deformation) reached 21 µm deep in the AM sample (Fig. 5a), while higher for the other two conditions, as 40 µm and 70 µm for the AM+LowPI (Fig. 5c) and AM+LargePI (Fig. 5e) conditions, respectively. It is also easy to see that due to the surface straining, multiple slip lines are enabled for all conditions. Additionally, this method enables the measurement of the heavily deformed layer (HDL) where most of the strain-induced recrystallisation (i.e., grain refinement) takes place. The HDL was measured as 1.6 µm, 2.1 µm and 3.5 µm for the AM, AM+LowPI and AM+LargePI conditions, respectively (Fig. 5b,d,f).

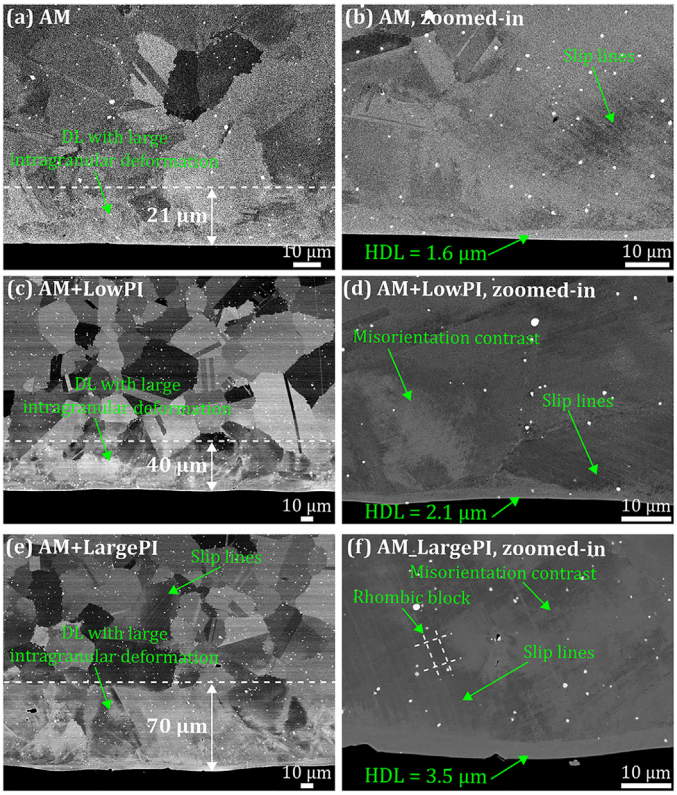

Fig. 5. Deformed layers (DL) with large intragranular deformation and heavily deformed layers (HDL) beneath the surface, assessed via BSEI.

While these metallurgical techniques complement the residual stress analysis (Fig. 3), they are intimately linked to the localised surface region upon which they were analysed from, which is why there is no clear consistency in the deformed layers measured with the different techniques (Table 1).

While the assessment of the misorientation depth is associated with the amount of dislocation motion and plastic deformation induced by the machining and peening processes, it remains insufficient to find its relation with more relevant aspects, such as material response under loading, which can be quite different near the deformed layer than in the bulk material [14,16]. Therefore, micromechanical testing shows potential for assessing the mechanical behaviour in the subsurface – this is discussed next.

Table 1
Depth measurements of the strain hardening layer (SHL) and deformed layers (DL) of the machined and peened conditions, as measured with different techniques.

Sample condition	SHL (µm), via XRD	HDL (µm), via SEM	DL (µm), via SEM	DL (µm), via EBSD
AM	100	1.6 ± 0.08	21±1.31	32±2.70
AM+LowPI	100	2.1 ± 0.16	40±2.43	11±0.69
AM+LargePI	200	3.5 ± 0.28	70±5.06	36±3.11

4. Role of shot peening on the micromechanics of the alloy

Microindentation, which has been employed extensively to assess the hardness in the subsurface of Ni-base superalloys, cannot provide the full micromechanical information, since due to the 'edge effect', indentations near the surface are not reliable [11], plus they do not straightforwardly enable an analysis of the strength or plastic behaviour of the material. Hence, micropillar compression testing was employed to tackle this aspect due to the simple uniaxial stress state that it comprises.

To characterise the machined and peened surfaces, micropillars were compressed at different depths, namely at the edge (at ~10 µm), 50 µm and 100 µm. It was ensured that pillars were inside single grains, thus knowing the crystal orientation for each pillar via EBSD (Fig. 1). This allows to calculate the critical resolved shear stress (CRSS) for all tests, and thus yields an objective comparison of micropillar strength regardless of the orientation of the grain's crystallographic planes. Based on the Euler angles (Φ_1, Φ, Φ_2), the CRSS (τ) for each pillar was calculated as [11]:

$$(\phi_1,\ \phi,\phi_2) \rightarrow \quad G_{mat}$$

$$For\ i \in [1,\ldots,12] \begin{cases} hkl_i = G_{mat} \times l_i \qquad \cos(\lambda)_i = \dfrac{z_{vec}\cdot hkl_i}{\| hkl_i \| \times \| z_{vec} \|} \\ uvw_i = G_{mat} \times n_i \qquad \cos(\psi)_i = \dfrac{z_{vec}\cdot uvw_i}{\| uvw_i \| \times \| z_{vec} \|} \\ \tau = \sigma \times \{ \max[\cos(\lambda)_i, \cos(\psi)_i\ ] \} \end{cases} \quad (1)$$

where G_{mat}, z_{vec}, σ, l_i, n_i and i, are the orientation matrix derived from the Euler angles, compression axis vector, axial stress, slip direction, slip plane, and slip system, respectively. The term $\max[\cos(\lambda)_i \cos(\psi)_i]$ is the Schmid factor of the grain in question, which for the 16 compressed micropillar locations was measured as 0.424±0.065, considering the {111}<110> slip system family.

All micropillars depicted a typical engineering stress-strain curve (Fig. 6a), characterised by either a serrated or non-serrated trend past the yield point, which is explained by the consecutive slipping process in which energy is accumulated before every slip along the primary slip system (Fig. 7b,c).

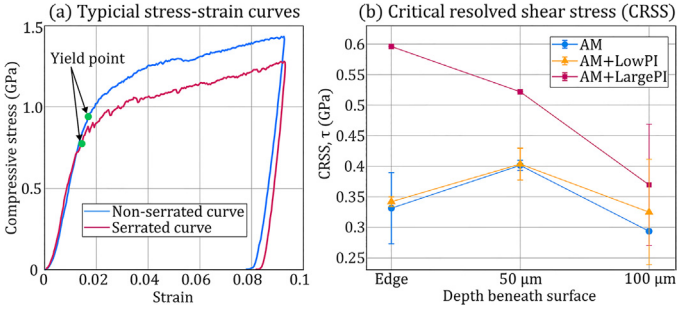

Fig. 6. Micropillar compression tests results. (a) Typical engineering stress-strain curves (examples from the AM+LowPI sample; the non-serrated and serrated curves correspond to 50 and 100 µm depths, respectively). (b) CRSS as a function of depth beneath the machined and peened surfaces for all conditions.

Near the edge, the AM+LargePI condition exhibited the largest CRSS (0.59 GPa), being about 77% larger than in the AM and AM +LowPI conditions; this could be explained due to the large number of dislocations induced at the surface at this large peening intensity. At 50 µm, the CRSS from the AM+LargePI sample reduces to 0.52 GPa, but it is still significantly larger (by 30%) than the other two conditions. At 100 µm, the CRSS from the AM+LargePI further reduces to 0.37 GPa, being only slightly larger than the AM (by 26%) and the AM +LowPI (by 14%). Thus, this highlights that the CRSS of the material is better enhanced by a larger peening intensity. Interestingly, however, the CRSS between the AM and the AM+LowPI condition is fairly the same at all depths beneath the surface, being only an 11% difference at a 100 µm depth.

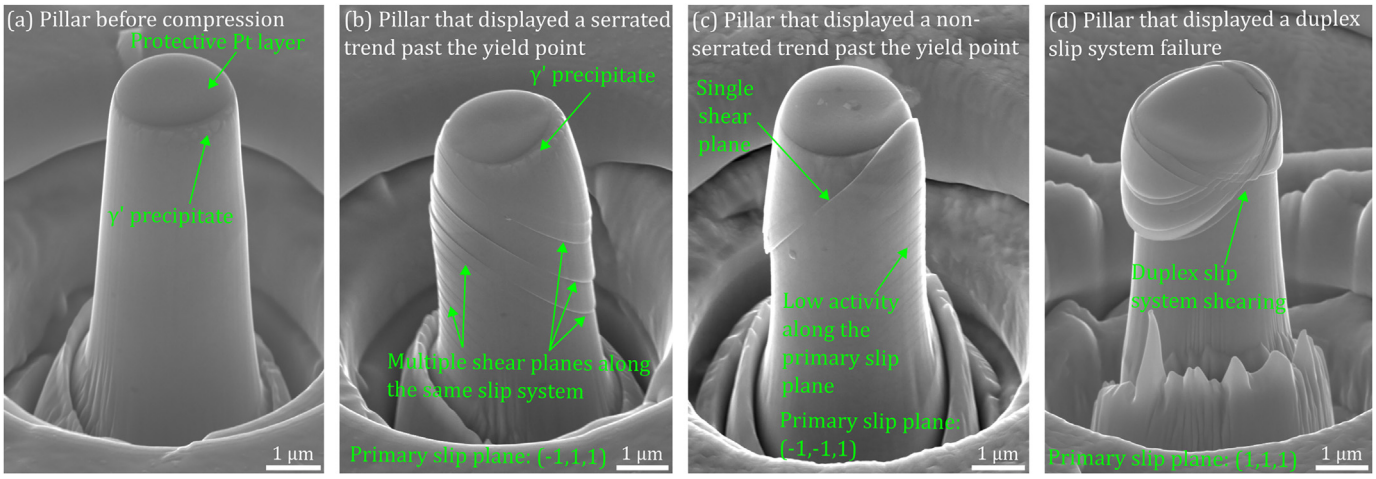

Fig. 7. Micropillar compression tests. (a) Micropillar before test. (b) Dominant failure mechanism with several active shear planes along the primary slip system. (c) Dominant failure mechanism with a single active shear plane and low activity in the same slip system. (d) Duplex slip system shearing failure.

These results prove that even while the residual stress profile may indicate that there is a compressive state of residual stress (Fig. 3), it does not necessarily imply a favourable shift in the micromechanical properties (i.e., yield, CRSS). This is likely due to the initial surface state (i.e., pre-strained under tension due to machining), aspect that is typically neglected in shot peening studies, where the surface is in pristine condition with insignificant surface anomalies. Here, more in line with an industrial process, the alloy already presented a heavily deformed layer before peening, due to the machining operation.

All pillars failed by shearing along a primary slip system (Fig. 7b-d). In some cases, multiple active shear planes were detected (Fig. 7b), while in some others there was a single active shear plane and low strain activity along the primary slip system without shearing (Fig. 7c). Only a minority of the pillars failed by displaying a duplex slip system shearing failure (Fig. 7d). No distinction of failure mode was identified between the surface conditions. This indicates that although different strengthened effects have been introduced by machining and shot peening processes, these do not adversely affect the failure mechanism at the microscale.

5. Conclusions

This paper reports the shot peening influence on the surface integrity of pre-strained (via machining) surfaces of a Ni-base superalloy. After machining and shot peening, usual assessment techniques (i.e., XRD, EBSD, SEM) were employed, but the measured deformed layers showed a high dependency on the location of measurement. Based on the residual stress profiles, it would be assumed that the low and large peening intensities favour the CRSS up to 100 µm and 200 µm deep, respectively. Nevertheless, following micropillar compression tests, it was revealed that the CRSS of the material is not enhanced by the low peening intensity at all, and that peening at large intensity does in fact significantly improve the CRSS of the material, but only up to about a 100 µm depth. This highlights that even while residual stresses are useful for identifying the overall surface state and quality, they might be deceiving as to the extent on which micromechanical behaviour could be enhanced. Moreover, the pre-strained condition of the material could also affect the result of the shot-peened surface. Therefore, traditional techniques to measure the effect of shot peening, such as XRD, EBSD and SEM, need to be complemented with additional techniques that allow a more in-depth evaluation, like micromechanical testing. While these results explored the role of shot peening on the CRSS via micropillar compression, the results from other types of micromechanical tests (e.g., microcantilever beam bending, micro-tensile) could also reveal new information based on the strain history of the material prior to shot peening.

Declaration of Competing Interest

The authors declare that they have no known competing financial interests or personal relationships that could have appeared to influence the work reported in this paper.

Acknowledgements

The authors thank and acknowledge Prof. Dragos Axinte, who spent significant effort on this work; Rolls-Royce plc for provision of material and financial support; and the nmRC for providing access to instrumentation.

References

[1] Reed R (2006) *The Superalloys*, Cambridge University PressCambridge.
[2] Soo S-L, Hood R, Aspinwall D-K, Voice W-E, Sage C (2011) Machinability and Surface Integrity of RR100 Nickel Based Superalloy. *CIRP Annals - Manufacturing Technology* 60(1):89–92.
[3] Liao Z, et al. (2021) Surface Integrity in Metal Machining - Part I: Fundamentals of Surface Characteristics and Formation Mechanisms. *International Journal of Machine Tools and Manufacture* 162:103687.
[4] Liao Z, et al. (2019) Grain Refinement Mechanism of Nickel-Based Superalloy by Severe Plastic Deformation - Mechanical Machining Case. *Acta Materialia* 180:2–14.
[5] Yeratapally S, Glavicic M, Hardy M, Sangid M (2016) Microstructure Based Fatigue Life Prediction Framework for Polycrystalline Nickel-Base Superalloys with Emphasis on the Role Played by Twin Boundaries In Crack Initiation. *Acta Materialia* 107:152–167.
[6] Sarikaya M, et al. (2021) A State-of-the-Art Review on Tool Wear and Surface Integrity Characteristics In Machining Of Superalloys. *CIRP-JMST* 35:624–658.
[7] la Monaca A, Liao Z, Axinte D, M'Saoubi R, Hardy M-C (2021) Towards Understanding the Thermal History of Microstructural Surface Deformation When Cutting a Next Generation Powder Metallurgy Nickel-Base Superalloy. *International Journal of Machine Tools and Manufacture* 168:103765.
[8] la Monaca A, Liao Z, Axinte D, M'Saoubi R, Hardy M-C (2021) Can Higher Cutting Speeds and Temperatures Improve the Microstructural Surface Integrity of Advanced Ni-base Superalloys? *CIRP Annals* 71(1):113–116.
[9] la Monaca A, et al. (2021) Surface Integrity in Metal Machining - Part II: Functional Performance. *International Journal of Machine Tools and Manufacture* 164:103718.
[10] Bandyopadhyay R, Sangid M-D (2019) Crystal Plasticity Assessment of Inclusion- and Matrix-Driven Competing Failure Modes in a Nickel-Base Superalloy. *Acta Materialia* 177:20–34.
[11] Messé OMD-M, Stekovic S, Hardy M-C, Rae CM-F (2014) Characterization of Plastic Deformation Induced by Shot-Peening in a Ni-Base Superalloy. *The Journal of The Minerals, Metals & Materials Society* 66:2502–2515.
[12] Jackson T-J, Rolph J, Buckingham R-C, Hardy M-C (2020) The Effect of Shot Peening on the Ductility and Tensile Strength of Nickel-Based Superalloy Alloy 720Li, Superalloys 2020. *The Minerals, Metals & Materials Series* : 535–545.
[13] Evans A, Kim S-B, Shackleton J, Bruno G, Preuss M, Withers P-J (2005) Relaxation of Residual Stress in Shot Peened Udimet 720Li Under High Temperature Isothermal Fatigue. *International Journal of Fatigue* 27(10–12):1530–1534.
[14] Axinte D, Huang H, Yan J, Liao Z (2022) What Micro-Mechanical Testing Can Reveal About Machining Processes. *International Journal of Machine Tools and Manufacture* 183:103964.
[15] Hardy, M., Reed, R., Crudden, D., 2019, Nickel-Base Superalloy. US10422024B2.
[16] Liao Z, Axinte D, Mieszala M, M'Saoubi R, Michler J, Hardy M (2018) On the Influence of Gamma Prime Upon Machining of Advanced Nickel Based Superalloy. *CIRP Annals* 67:109–112.